

The transcriptional hub *SHORT INTERNODES1* integrates hormone signals to orchestrate rice growth and development

Erchao Duan ^{1,†} Qibing Lin ^{2,†} Yihua Wang ^{1,†} Yulong Ren ² Huan Xu ¹ Yuanyan Zhang ¹ Yunlong Wang ¹ Xuan Teng ¹ Hui Dong ¹ Yupeng Wang ² Xiaokang Jiang ¹ Xiaoli Chen ¹ Jie Lei ¹ Hang Yang ¹ Rongbo Chen ¹ Ling Jiang ¹ Haiyang Wang ² and Jianmin Wan ^{1,2,*}

- 1 State Key Laboratory of Crop Genetics and Germplasm Enhancement and Utilization, Jiangsu Plant Gene Engineering Research Center, Nanjing Agricultural University, Nanjing 210095, China
- 2 State Key Laboratory of Crop Gene Resources and Breeding, Institute of Crop Sciences, Chinese Academy of Agricultural Sciences, Beijing 100081, China

*Author for correspondence: wanjm@njau.edu.cn, wanjianmin@caas.cn

[†]These authors contributed equally.

The author responsible for distribution of materials integral to the findings presented in this article in accordance with the policy described in the Instructions for Authors (<https://academic.oup.com/plcell/pages/General-Instructions>) is: Jianmin Wan (wanjm@njau.edu.cn or wanjianmin@caas.cn).

Abstract

Plants have evolved sophisticated mechanisms to coordinate their growth and stress responses via integrating various phytohormone signaling pathways. However, the precise molecular mechanisms orchestrating integration of the phytohormone signaling pathways remain largely obscure. In this study, we found that the rice (*Oryza sativa*) *short internodes1* (*shi1*) mutant exhibits typical auxin-deficient root development and gravitropic response, brassinosteroid (BR)-deficient plant architecture and grain size as well as enhanced abscisic acid (ABA)-mediated drought tolerance. Additionally, we found that the *shi1* mutant is also hyposensitive to auxin and BR treatment but hypersensitive to ABA. Further, we showed that OsSHI1 promotes the biosynthesis of auxin and BR by activating the expression of *OsYUCCAs* and *D11*, meanwhile dampens ABA signaling by inducing the expression of *OsNAC2*, which encodes a repressor of ABA signaling. Furthermore, we demonstrated that 3 classes of transcription factors, AUXIN RESPONSE FACTOR 19 (*OsARF19*), LEAF AND TILLER ANGLE INCREASED CONTROLLER (*LIC*), and *OsZIP26* and *OsZIP86*, directly bind to the promoter of *OsSHI1* and regulate its expression in response to auxin, BR, and ABA, respectively. Collectively, our results unravel an *OsSHI1*-centered transcriptional regulatory hub that orchestrates the integration and self-feed-back regulation of multiple phytohormone signaling pathways to coordinate plant growth and stress adaptation.

Introduction

Plants are affected by a myriad of biotic and abiotic signals and must constantly adapt their growth and development to fluctuating environmental conditions to guarantee survival and reproduction with optimal resource reallocation (Huot et al. 2014; Zhang et al. 2020). Several classes of phytohormones play a critical role in regulating the balance of various developmental process and stress adaptation, through signal transduction and integration at different levels, including transcriptional,

posttranscriptional, and epigenetic levels (Achard et al. 2006; Chaiwanon et al. 2016; Waadt et al. 2022). Unraveling the molecular mechanisms of signaling integration of various hormone signaling pathways is a fundamental biological question, which also has important implications for molecular breeding of high-yielding and stress-resilient crops.

Among the known hormones, auxin, and brassinosteroids (BRs) are generally regarded as growth-promoting hormones, whereas abscisic acid (ABA) is regarded as a stress-responsive

IN A NUTSHELL

Background: Plant growth and development are affected by various internal and external signals during their entire life cycle. To improve their chances of surviving and reproducing, plants have evolved complex ways to coordinate their growth and stress responses via integrating hormone signaling pathways. Therefore, revealing the molecular mechanisms integrating various hormone signaling pathways is not only a fundamental biological question but also holds a great promise for molecular breeding of high-yielding and stress-resilient crops in face of climate change and increasing human population.

Questions: The multifaceted hormone-related defects of the rice *short internodes1* (*shi1*) mutant give us a clue that the *OsSHI1* gene might participate in regulating multiple hormone signaling pathways. Therefore, we asked whether and how different hormone signaling pathways are integrated by *OsSHI1* at the transcriptional level during rice development.

Findings: We found that the *shi1* mutant exhibits many hormone-related morphological variations, such as auxin and brassinosteroid (BR)-regulated plant development as well as abscisic acid (ABA)-mediated stress tolerance. Further functional analysis revealed that several upstream transcription factors of auxin, ABA, and BR pathways bind to the promoter region of *OsSHI1* to activate or inhibit its transcription. OsSHI1 protein then directly regulates several auxin and BR biosynthesis genes, thus integrating the biosynthesis of auxin and BR with ABA signal transduction to coordinate plant growth and stress adaptation. In addition, *OsSHI1* also negatively regulates its own expression. These findings demonstrate that OsSHI1 is a key transcriptional hub for the integration of multiple hormone signaling pathways.

Next steps: SHI family members are essential regulators of plant development. Therefore, it is important to identify and explore their functions in other hormone pathways or stresses to fully understand the biological functions of SHI transcription factors in coordinating plant development and stress adaptation in future studies.

hormone (Huot et al. 2014; Chaiwanon et al. 2016; Li et al. 2021). Auxin is mainly produced through the classical 2-step indole-3-pyruvic acid (IPA) pathway controlled by the YUCCA (YUC) family of flavin monooxygenases (Zhao 2010). Auxin perception triggers the activation of AUXIN RESPONSE FACTOR (ARF) proteins to regulate downstream transcriptional programs by binding to the auxin-responsive *cis*-regulatory elements (AuxREs) (Wagner and Weijers 2016). BRs are derived from campesterol through a succession of reactions catalyzed by different members of the cytochrome P450 (CYP450) monooxygenase family (DWARF2, DWARF11 [D11], etc.) (Fujioka and Yokota 2003; Hong et al. 2005; Tanabe et al. 2005). BR induces a cascade of phosphorylation and dephosphorylation events to regulate diverse downstream transcription factors required for optimal BR responses, such as BRASSINAZOLE-RESISTANT1 (BZR1), LEAF AND TILLER ANGLE INCREASED CONTROLLER (LIC), DWARF AND LOW-TILLERING (DLT), and REDUCED LEAF ANGLE1 (RLA1) (Kim and Wang 2010; Tong and Chu 2018).

ABA is an isoprenoid-derived phytohormone that accumulates during seed maturation and in response to various environmental stresses (Nambara and Marion-Poll 2005). ABA signal transduction ultimately phosphorylates downstream ABA-responsive transcription factors (such as bZIP proteins) and membrane channels to combat environmental stresses (Raghavendra et al. 2010). Although previous studies have documented signaling integration of auxin, BR, and ABA through protein–protein interaction or phosphorylation of key components from each pathway (Cai et al. 2014; Gui

et al. 2016; Wang, Tang, et al. 2018; Zhao et al. 2019), how their signaling pathways integrate at the transcriptional level remains largely obscure.

We previously reported that rice (*Oryza sativa*) SHORT INTERNODES1, a member of the plant-specific SHI transcription factor family, plays a pleiotropic role in regulating rice development, such as rice tillering (Duan et al. 2019). In this study, we further show that malfunction of *OsSHI1* confers multiple hormone-related phenotypic effects during the entire plant life cycle. Our molecular and genetic evidence demonstrates that OsSHI1 acts as a key transcriptional hub mediating the integration and self-feedback regulation of auxin, BR, and ABA pathways at the transcriptional level to coordinately regulate plant growth and stress responses in rice.

Results

Hormone-related pleiotropic phenotypes of *Ossh1* mutants and overexpressors *OsSHI1*

We previously reported that OsSHI1 regulates plant architecture by repressing the transcriptional activity of SQUAMOSA PROMOTER BINDING PROTEIN-LIKE 14 (*OsSPL14*) (also named IDEAL PLANT ARCHITECTURE 1 [IPA1]) in rice (Duan et al. 2019). We noticed that besides the reduced tiller and increased panicle branch number, the *shi1* mutant also exhibits pleiotropic hormone-related morphological defects during the entire life cycle. For instance, consistent with the high expression level of *OsSHI1* in young root tissue (Duan et al. 2019), the young *shi1* plants exhibited reduced

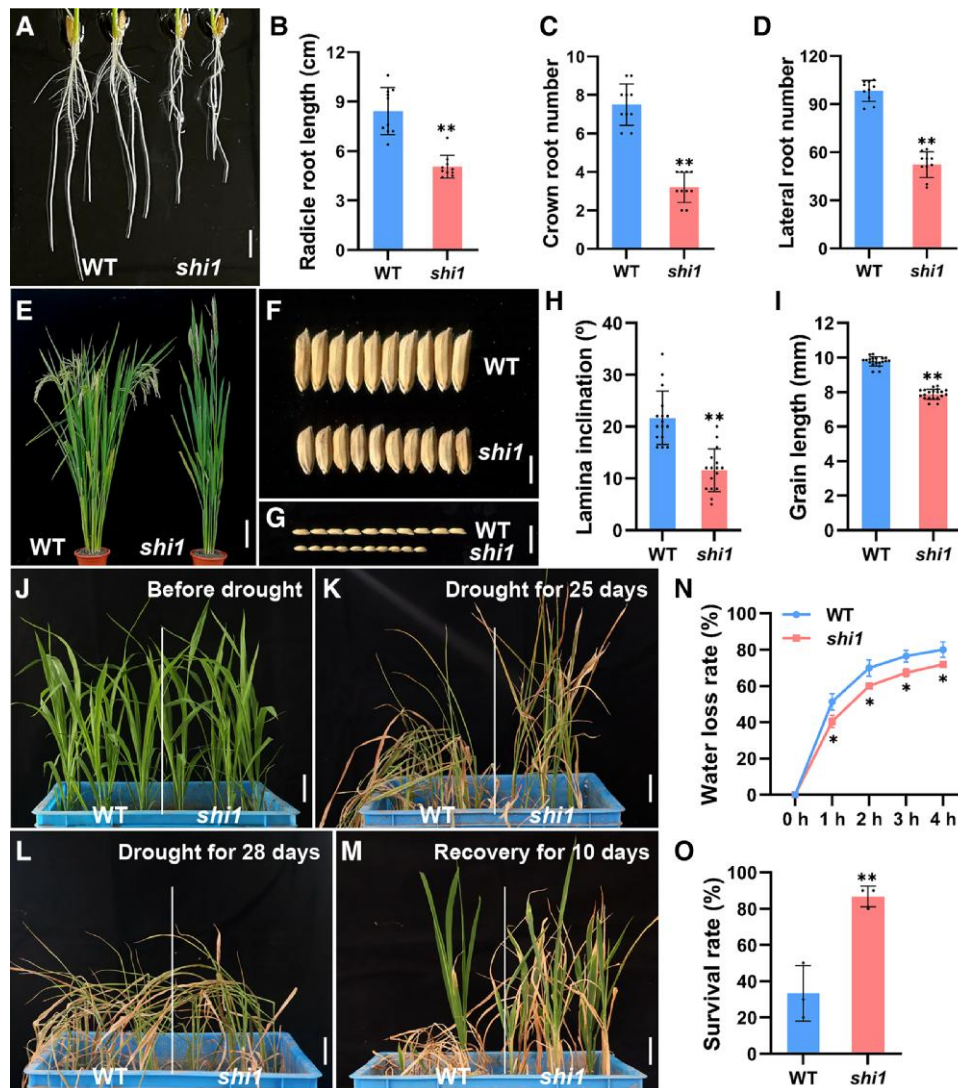


Figure 1. Pleiotropic phenotypes of the *OsSHI1*-deficient mutant *shi1* compared to WT. **A)** Root morphology of 1-wk-old WT and *shi1* plants grown in liquid MS medium. Bar = 1 cm. **B to D)** Radicle root length **B)**, crown root number **C)**, and lateral root number **D)** of 1-wk-old WT and *shi1* plants ($n = 10$ plants). **E)** Phenotypes of WT and *shi1* plants at the mature stage. Bar = 20 cm. **F, G)** Mature grain morphology of WT and *shi1* plants. Bars = 5 mm in **F)** and 1.5 cm in **G)**. **H, I)** Lamina inclination and grain length of WT and *shi1* plants at the mature stage ($n = 16$ plants and 20 grains, respectively). **J to M)** Drought tolerance testing of 1-mo-old WT and *shi1* plants ($n = 3$, 10 plants for each repeat). Bars = 6 cm. **N)** Water loss rate of fully expanded leaves of 1-mo-old WT and *shi1* plants ($n = 3$). Water loss was expressed as a percentage relative to the total water content. **O)** Survival rate of 1-mo-old WT and *shi1* plants underwent drought stress ($n = 3$). Values are means \pm SD, and the statistically significant differences were determined by Student's *t*-test (* $P < 0.05$ and ** $P < 0.01$) in **B to D)**, **H)**, **I)**, **N)**, and **O)**.

radicle root length, crown, and lateral root numbers (Fig. 1, A to D), reminiscent of auxin-deficient root phenotypes (Wang, Zhang, et al. 2018). In contrast, the *OsSHI1* overexpressors, *ProUbi:OsSHI1* transgenic plants, had increased crown and lateral root numbers but comparable radicle root length, compared to wild-type (WT) Nipponbare (Nip) when grown on Murashige and Skoog (MS) medium (Supplemental Fig. S1, A to D).

In addition, the mature *shi1* plants displayed typical BR-deficient phenotypes, such as dark-green leaves, compact plant architecture as well as reduced grain size (Fig. 1, E to I; Duan et al. 2019), while the *ProUbi:OsSHI1* transgenic plants

had typical BR-enhanced phenotypes, such as reduced plant height, drooping leaves, and smaller grain compared to the WT (Supplemental Fig. S1, E to J). Moreover, we found that when subjected to drought stress, the *shi1* mutant plants had reduced water loss rate and thereby elevated survival rates (Fig. 1, J to O), while the *ProUbi:OsSHI1* transgenic plants had significantly decreased survival rates compared to the WT (Supplemental Fig. S1, K to N). These results indicate that *OsSHI1* promotes root development and BR-mediated growth but represses drought tolerance, suggesting that *OsSHI1* is likely involved in multiple hormone signaling pathways.

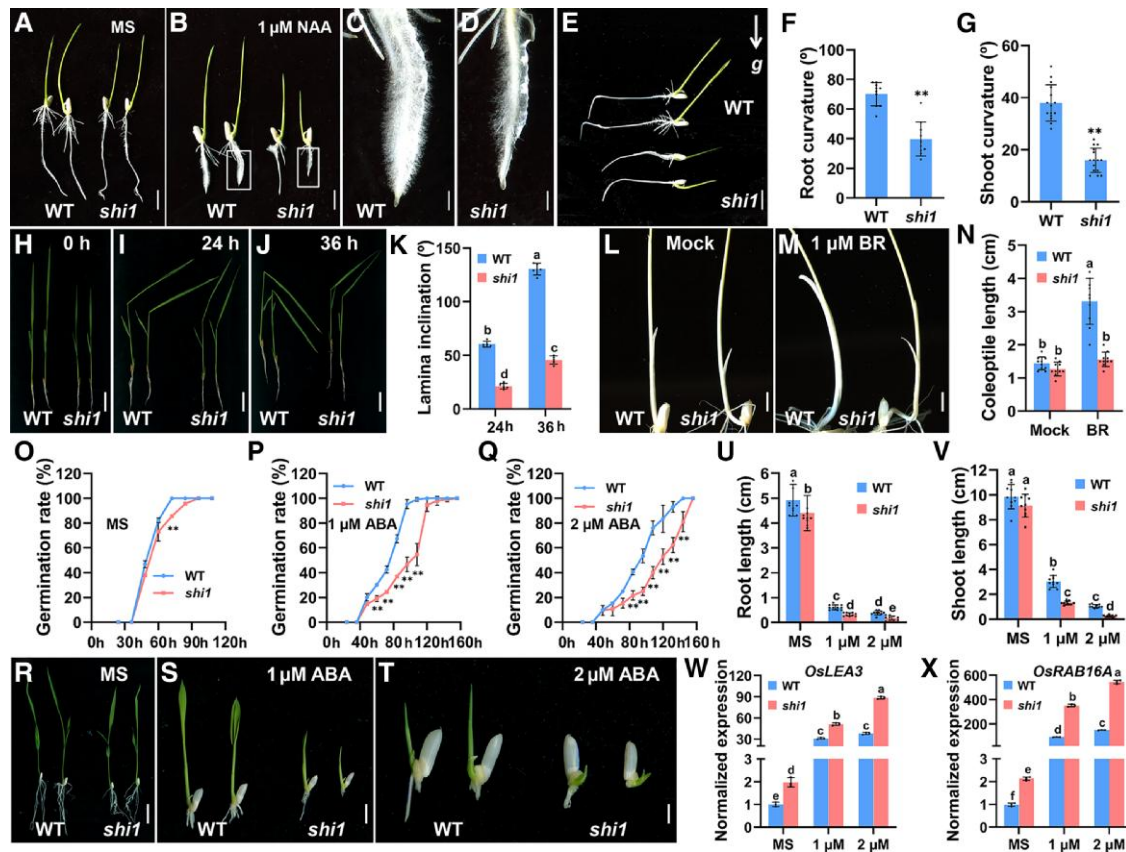


Figure 2. Responses of WT and *shi1* to NAA, ABA, and BR treatments. **A to D)** Root hair phenotypes of WT and *shi1* plants treated with 0 (MS), 1 μ M naphthylacetic acid (NAA) for 3 d. **C, D)** are enlarged images of the boxed regions in **B)**. Bars = 1 cm in **A)**, 6 mm in **B)**, and 1 mm in **C)** and **D)**. **E to G)** Gravitropic responses of WT and *shi1* plants for 3 h ($n = 10$ plants). Bar = 1 cm. **H to K)** Lamina inclination of WT and *shi1* plants treated with 1 μ M BR for 24 and 36 h ($n = 10$ plants). Bars = 4 cm. **L to N)** Coleoptile phenotypes of WT and *shi1* upon 0 **L)** and 1 μ M BR **M)** treatment for 1 wk in darkness ($n = 10$ plants). Bars = 4 mm. **O to Q)** Germination rates of WT and *shi1* seeds treated with 0 (MS) **O)**, 1 μ M **P)**, and 2 μ M ABA **Q)** for 7 d ($n = 3$, 30 grains for each repeat). **R to V)** Growth phenotypes of WT and *shi1* plants treated with 0 (MS), 1, and 2 μ M ABA for 4 d ($n = 10$ plants). Bars = 1.5 cm in **R)**, 1 cm in **S)**, and 5 mm in **T)**. **W, X)** Relative expression levels of *OsLEA3* **W)** and *OsRAB16A* **X)** in WT and *shi1* plants treated with 0, 1, and 2 μ M ABA for 4 d ($n = 3$). *UBIQUITIN* gene was used as the endogenous control, and relative expression levels were normalized to *UBIQUITIN* which was set as 1. Values are means \pm SD, and the statistically significant differences were determined by Student's *t*-test (** $P < 0.01$) in **F)**, **G)**, and **O to Q)** or 2-way ANOVA in **K)**, **N)**, and **U to X)**.

To test this, we compared the responses of WT, *shi1*, and *OsSHI1* overexpression plants to treatments of exogenous auxin, BRs, and ABA. The results showed that auxin-stimulated root hair formation and root and shoot gravitropic responses were weakened in the *shi1* mutant (Fig. 2, A to G), but the auxin-stimulated root hair formation was substantially enhanced in the *ProUbi:OsSHI1* transgenic plants (Supplemental Fig. S2, A to H). In addition, the *shi1* mutant and the *ProUbi:OsSHI1* transgenic plants exhibited opposite responses to BR in the lamina inclination assay (Figs. 2, H to K, and S2, I to N) and BR treatment hardly promoted coleoptile elongation of the *shi1* mutant (Fig. 2, L to N). Moreover, the *shi1* mutant displayed reduced seed germination rate but hypersensitivity to ABA treatment with respect to inhibited seedling growth as well as elevated expression levels of 2 representative ABA-responsive genes *LATE EMBRYOGENESIS ABUNDANT 3* (*OsLEA3*) and *RESPONSIVE TO ABSCISIC ACID 16A* (*OsRAB16A*) (Fig. 2, O

to X), while the *ProUbi:OsSHI1* transgenic plants exhibited opposite responses (Supplemental Fig. S2, O to X). These observations collectively demonstrate that the *shi1* mutant had reduced response to auxin and BR, and increased response to ABA. Conversely, the *ProUbi:OsSHI1* transgenic plants display enhanced responses to auxin and BR and a decreased response to ABA.

OsSHI1 regulates auxin and BR biosynthesis and ABA signaling pathways

To investigate how *OsSHI1* affects the biosynthesis or signaling pathways of auxin, BR, and ABA, we first quantified the contents of these hormones using HPLC. The contents of auxin and the BR upstream intermediates typhasterol (TY) and castasterone (CS) as well as ABA were dramatically decreased (by 59.3% for auxin, 83.5% for TY, 79.4% for CS, and 50.4% for ABA) in the *shi1* mutant (Figs. 3, A and B, and S3A).

In agreement with the reduced levels of auxin and BRs, the transcript levels of *OsYUCCAs* and *D11*, which encode enzymes catalyzing the rate-limiting step in auxin and BR biosynthesis, respectively (Tanabe et al. 2005; Yamamoto et al. 2007), were significantly reduced in *shi1* (Fig. 3C), suggesting that OsSHI1 participates in the biosynthesis of auxin and BR.

Unexpectedly, we found that ABA content was also decreased in the *shi1* mutant (Supplemental Fig. S3A), whereas its ABA sensitivity and drought resilience were significantly increased (Fig. 1, J to O and O to X). Reverse transcription quantitative PCR (RT-qPCR) analysis showed that the expression levels of most ABA biosynthetic genes, such as *ABA-deficient* (*OsABA1-4*) and *9-cis-epoxycarotenoid dioxygenase* (*OsNCED1-5*), were not significantly altered in the *shi1* mutant. Consistent with this result, a yeast 1-hybrid (Y1H) assay showed that OsSHI1 does not bind to the promoters of ABA biosynthetic genes (Supplemental Fig. S3, B and C). These observations suggest that OsSHI1 likely indirectly affects ABA biosynthesis and that ABA signaling was likely enhanced in *shi1*.

Consistent with this speculation, we observed reduced expression of *OsNAC2* (a negative regulator of ABA signaling; Shen et al. 2017) in the *shi1* mutant (Fig. 3D). Additionally, we also observed that the expression levels of *OsLEA3* and *RESPONSIVE TO ABSCISIC ACID 21* (*OsRAB21*), 2 positive ABA responsive genes negatively regulated by *OsNAC2* (Shen et al. 2017), were upregulated in the *shi1* mutant (Fig. 3D), indicating that *OsSHI1* may act in the same pathway with *OsNAC2*.

We further performed transient dual-LUC assay in rice protoplasts to evaluate the regulatory effect of OsSHI1 on the transcriptional activity of *OsYUCCAs*, *D11*, and *OsNAC2*. Consistent with reduced transcript abundances of *OsYUCCAs*, *D11*, and *OsNAC2* in *shi1*, OsSHI1 significantly enhanced the expression of the *luciferase* (*LUC*) reporter gene driven by the promoters of *OsYUCCAs*, *D11*, and *OsNAC2* (Fig. 3E).

Intriguingly, motif scanning analysis identified the existence of numerous OsSHI1 recognition motifs (ACTCTAC-like) in the promoter regions of *OsYUCCAs*, *D11*, and *OsNAC2* (Supplemental Fig. S4), indicating that they are potential direct downstream targets of OsSHI1. In support of this notion, Y1H assay confirmed that OsSHI1 could bind directly to the promoters of *OsYUCCAs*, *D11*, and *OsNAC2* in yeast (*Saccharomyces cerevisiae*) cells but not to the mutated promoters with changed OsSHI1 recognition motifs (Figs. 3F and S5).

Chromatin immunoprecipitation-quantitative PCR (ChIP-qPCR) analyses with anti-OsSHI1 specific polyclonal antibodies also verified the recruitment of OsSHI1 by the promoter regions of *OsYUCCAs*, *D11*, and *OsNAC2* in vivo (Fig. 3G). In addition, electrophoretic mobility shift assay (EMSA) validated that OsSHI1 could specifically bind to the ACTCTAC-like motifs in the promoter regions of *OsYUCCAs*, *D11*, and *OsNAC2* (Figs. 3, H to L, and S6). Moreover, nonlabeled competing probes could effectively

reduce the binding ability of OsSHI1 in a dosage-dependent manner and mutation of the core sequence abolished the binding (Fig. 3, H to L). These results suggest that OsSHI1 directly regulates auxin and BR biosynthesis and ABA signaling pathways by activating the transcription of *OsYUCCAs*, *D11*, and *OsNAC2*, respectively.

OsSHI1 functions upstream of *OsYUCCAs*, *D11*, and *OsNAC2*

To test the genetic relationship between *OsSHI1* and downstream target genes, we performed further genetic analyses. Firstly, *OsSHI1* was overexpressed in *d11-2*, a weak BR-deficient mutant harboring a mutation in *D11* and its WT ZH11. We found that overexpression of *OsSHI1* (*ProUbi:OsSHI1/ZH11*) conferred a loose plant architecture, drooping leaves and slender grains, and that these effects were suppressed by defective *d11* in *ProUbi:OsSHI1/d11-2* (Figs. 4, A to D, and S7A). Moreover, we generated *shi1*, *d11* single mutants, and *d11 shi1* double mutants using the CRISPR/Cas9 approach (Supplemental Fig. S7B) and found that the *d11 shi1* double mutant displayed a similar phenotype (such as reduced plant height, smaller grain, and compact plant architecture) to the *d11* mutant (Fig. 4, E to H).

In addition, we also generated the *nac2* single and *nac2 shi1* double mutants with the CRISPR/Cas9 technology (Supplemental Fig. S7C). Phenotype observation and expression analyses revealed that the *nac2 shi1* double mutant exhibited higher sensitivity to ABA, similar to *nac2* (Fig. 4, I to N). Besides, similar to *shi1*, the *yucca1* mutant also displayed evident reduced root length and lateral root number (Supplemental Fig. S8), suggesting that *OsSHI1* and *OsYUCCA1* likely act in the same pathway to regulate root development. In all, these molecular and genetic results demonstrate that *OsSHI1* functions upstream of *OsYUCCAs*, *D11*, and *OsNAC2* to enhance BR responses but repress ABA responses.

OsSHI1 is regulated by auxin, BR, and ABA

Hormone treatment analyses suggest that the *shi1* mutant was hyposensitive to auxin and BR but hypersensitive to ABA (Figs. 2 and S2), indicating that *OsSHI1* is likely involved in the signaling pathways of these hormones. To investigate how *OsSHI1* participates in auxin, BR, and ABA signaling, we firstly examined the responses of *OsSHI1* gene to these hormones. RT-qPCR analysis showed that auxin and ABA induced while BR repressed accumulation of the *OsSHI1* transcript (Fig. 5A), indicating that expression of *OsSHI1* is subject to feedback regulation by the auxin, BR, and ABA signaling pathways.

To illustrate how *OsSHI1* is regulated by these hormones, we scanned the upstream promoter region of *OsSHI1* and found 3 AuxREs, 7 CTCGC, and 3 G-box motifs (Figs. 5B and S9). AuxRE is the binding motif for ARFs, the CTCGC motif is bound by a transcription factor named LIC, while the G-box is a known binding motif for bZIP transcription factors

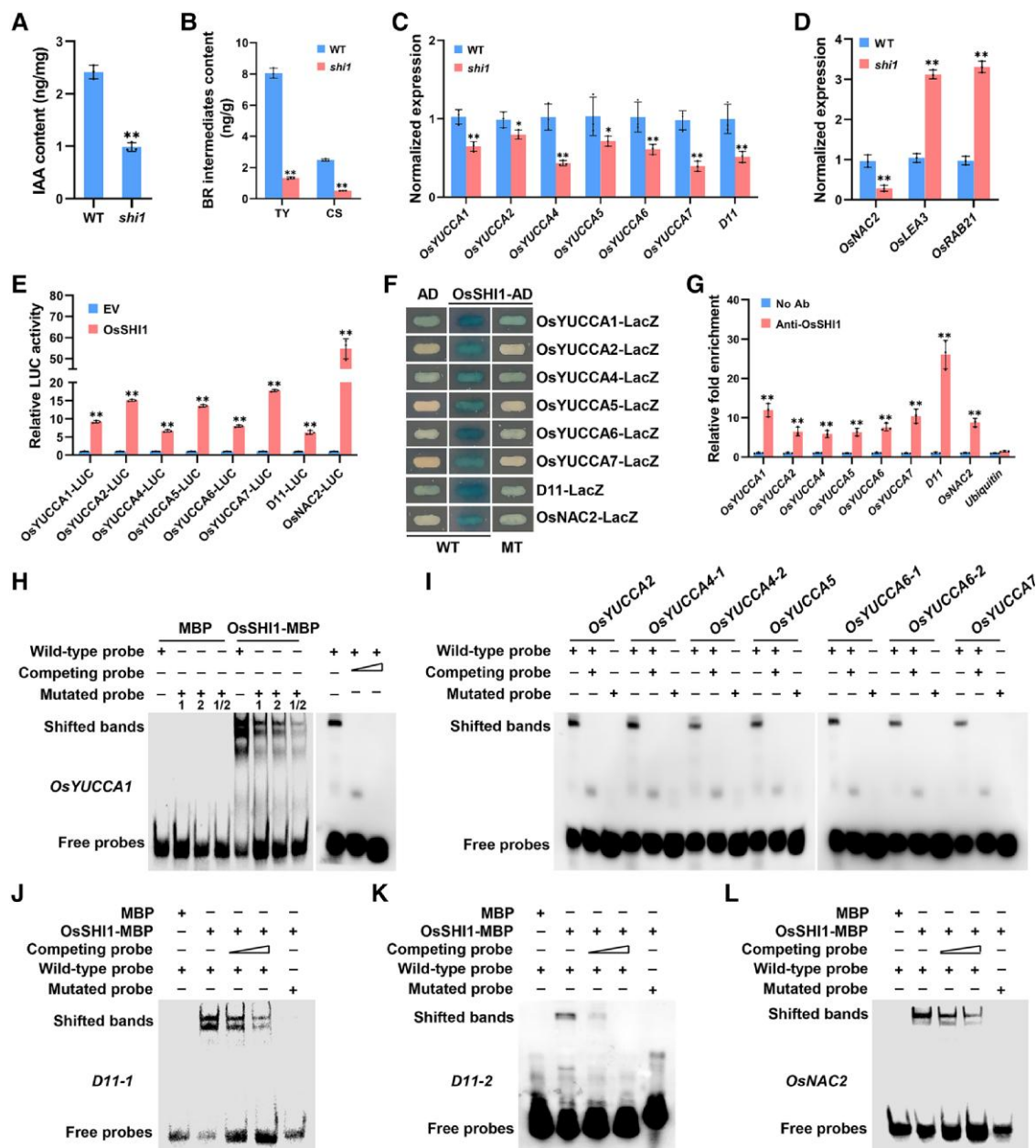


Figure 3. OsSHI1 regulates auxin and BR biosynthesis as well as ABA signaling pathway. **A)** IAA contents in 10-d-old WT and *shi1* plants ($n = 3$). **B)** TY and CS contents in 10-d-old WT and *shi1* plants ($n = 3$). **C)** Transcriptional levels of key genes involved in the biosynthesis of auxin and BR in WT and *shi1* plants ($n = 3$). *UBIQUITIN* gene was used as the endogenous control, and relative expression levels were normalized to *UBIQUITIN* which was set as 1. **D)** Expression levels of *OsNAC2* and ABA responsive genes *OsLEA3* and *OsRAB21* in WT and *shi1* plants ($n = 3$). *UBIQUITIN* gene was used as the endogenous control, and relative expression levels were normalized to *UBIQUITIN* which was set as 1. **E)** OsSHI1 activates the transcriptional activity of *OsYUCCAs*, *D11*, and *OsNAC2* in rice protoplasts. Relative LUC activity was calculated by LUC/Ren and normalized to that of empty vector (EV) control which was set as 1 ($n = 3$). **F)** Y1H assay shows that OsSHI1 directly binds to the promoter regions of 6 *OsYUCCA* genes, *D11*, and *OsNAC2*. The empty pB42AD vector (AD) was used as the negative control. WT, wild-type promoters of *OsYUCCAs*, *D11*, and *OsNAC2*. MT, mutated promoters of *OsYUCCAs*, *D11*, and *OsNAC2* in which the OsSHI1 recognition motifs were mutated. **G)** ChIP-qPCR analyses verify the binding of OsSHI1 to the promoter regions of *OsYUCCAs*, *D11*, and *OsNAC2* ($n = 3$). The fold enrichment was calculated as IP/Input. *Ubiquitin* was used as the negative control. No Ab, no antibody. **H to L)** EMSA confirms that OsSHI1 binds to the ACTCTAC-like motifs in the promoter regions of *OsYUCCA1* **H)**, other *OsYUCCAs* **I)**, *D11* **J)**, **K)**, and *OsNAC2* **L)**. MBP protein was used as the negative control. – and + indicate the absence and presence of the corresponding proteins or probes. The triangles indicate increased amounts of competing probes. 1 and 2 represent the first and second OsSHI1 recognition motifs in the *OsYUCCA1* promoter region. WT and mutated probes stand for oligonucleotides containing the native or mutated OsSHI1 recognition motifs in promoter regions of downstream target genes. See specific motifs at [Supplemental Fig. S4](#). Values are means \pm SD, and the statistically significant differences were determined by Student's *t*-test (* $P < 0.05$ and ** $P < 0.01$) in **A to E)** and **G)**.

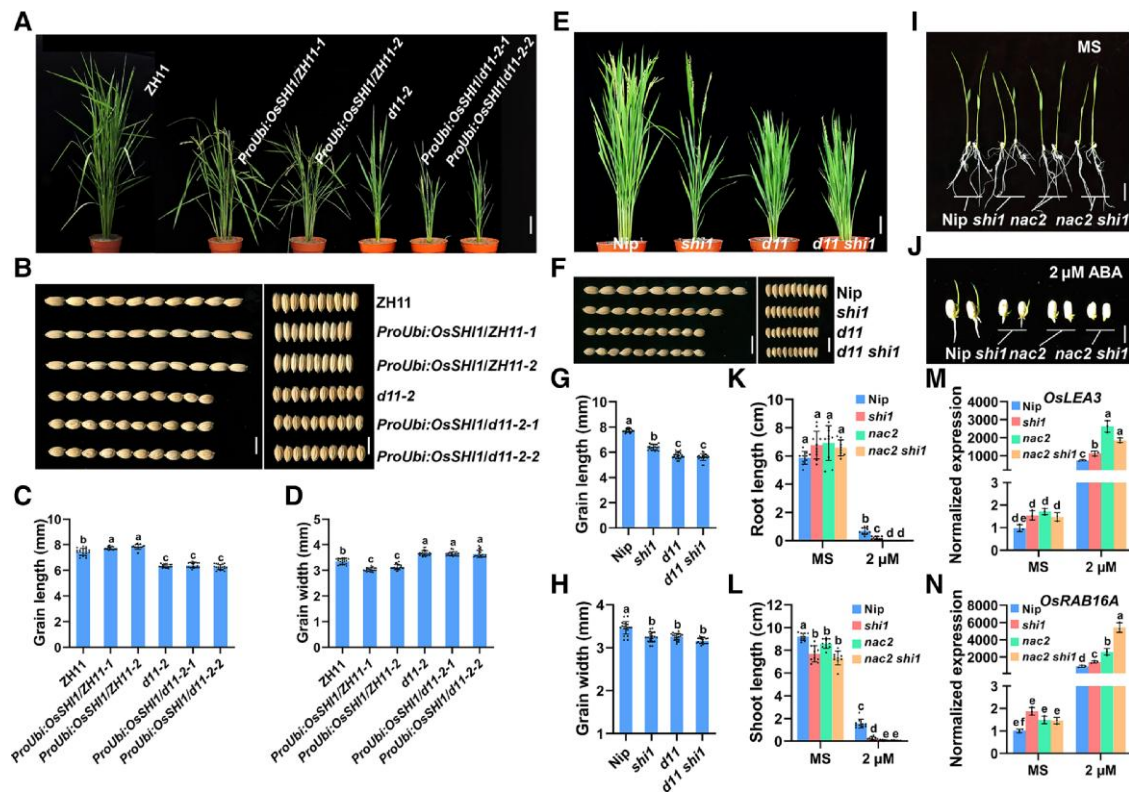


Figure 4. *OsSHI1* functions upstream of *D11* and *OsNAC2*. **A to D)** Plant architecture **A)**, grain size **B)**, grain length **C)**, and width **D)** of ZH11, *d11-2* mutant, and different *ProUbi:OsSHI1* transgenic lines in ZH11 and *d11-2* mutant backgrounds, respectively. Bar = 6 cm in **A)** and 6 mm in **B)**. $n = 20$ grains in **C)** and **D)**. **E to H)** Plant architecture **E)**, grain size **F)**, grain length **G)**, and width **H)** of Nip, *shi1*, *d11*, and *d11 shi1* mutant plants. Bars = 8 cm in **E)** and 8 mm in **F)**. $n = 20$ grains in **G)** and **H)**. **I, J)** Growth phenotypes of Nip, *shi1*, *nac2*, and *nac2 shi1* mutant plants treated with 0 (MS) **I)** and 2 μM ABA **J)** for 4 d, respectively. Bars = 1 cm in **I)** and 5 mm in **J)**. **K, L)** Root **K)** and shoot **L)** lengths of Nip, *shi1*, *nac2*, and *nac2 shi1* mutant plants treated with 0 and 2 μM ABA, respectively ($n = 10$ plants). **M, N)** Relative expression levels of *OsLEA3* **M)** and *OsRAB16A* **N)** in Nip, *shi1*, *nac2*, and *nac2 shi1* mutant plants treated with 0 and 2 μM ABA, respectively ($n = 3$). *UBIQUITIN* gene was used as the endogenous control, and relative expression levels were normalized to *UBIQUITIN* which was set as 1. Values are means \pm SD, and the statistically significant differences were determined by 2-way ANOVA in **C)**, **D)**, **G)**, **H)**, and **K to N)**.

(Wagner and Weijers 2016; Raghavendra et al. 2010; Zhang et al. 2012). To test whether these *cis*-elements mediate transcriptional regulation of *OsSHI1* by auxin, BR, and ABA, we cloned all of the open reading frames (ORFs) of the 25 *OsARFs*, *LIC*, and 89 *OsZIPs* in rice (Wang et al. 2007; Zhang et al. 2012; Zg et al. 2014).

Y1H assays revealed that *OsARF12*, *OsARF17*, *OsARF19*, *OsARF25*, *LIC*, *OsZIP26*, and *OsZIP86* could bind directly to the promoter of *OsSHI1* in yeast cells (Figs. 5C and S10). Further Y1H assays identified the F2 fragment of *OsSHI1* promoter as the potential platform for recruitment of *LIC* (Supplemental Fig. S11). EMSA confirmed that *OsARF12*, *OsARF17*, *OsARF19*, and *OsARF25* predominantly bound to the first AuxRE motif while *LIC* bound directly to the CTCGC motif in the F2 fragment and *OsZIP26* and *OsZIP86* bound specifically to the third G-box motif (Figs. 5, D to G, and S12). The nonlabeled competing probes could effectively reduce the binding ability of *OsSHI1* in a dosage-dependent manner and mutation of the core sequence abolished the binding (Fig. 5, D to G). Furthermore, ChIP-qPCR

assay with the *Pro35S:OsARF19-FLAG*, *Pro35S:LIC-GFP*, *Pro35S:OsZIP26-FLAG*, and *Pro35S:OsZIP86-FLAG* transgenic plants verified the enrichment of these binding sites by *OsARF19*, *LIC*, *OsZIP26*, and *OsZIP86* in vivo (Fig. 5, H to J). These observations suggest that *OsARF12*, *OsARF17*, *OsARF19*, *OsARF25*, *LIC*, *OsZIP26*, and *OsZIP86* may directly mediate the transcriptional regulation of *OsSHI1* by auxin, BRs, and ABA, respectively.

OsARF12, *OsARF17*, *OsARF25*, and especially *OsARF19* are evolutionarily closely related with *Arabidopsis* (*Arabidopsis thaliana*) *AtARF7* and *AtARF19* (Supplemental Fig. S13A), 2 ARF transcription factors that play crucial roles regulating root development in *Arabidopsis* (Okushima et al. 2007). Notably, all of them belong to the class A type ARFs characterized by the presence of a glutamine (Q)-rich middle region that confers transcriptional activation (Ulmasov et al. 1999) (Supplemental Fig. S13B). RT-qPCR assay showed that the expression levels of *OsARF12*, *OsARF17*, *OsARF19*, and *OsARF25* were all induced by exogenous naphthylacetic acid (NAA) treatment (Supplemental Fig. S13C).

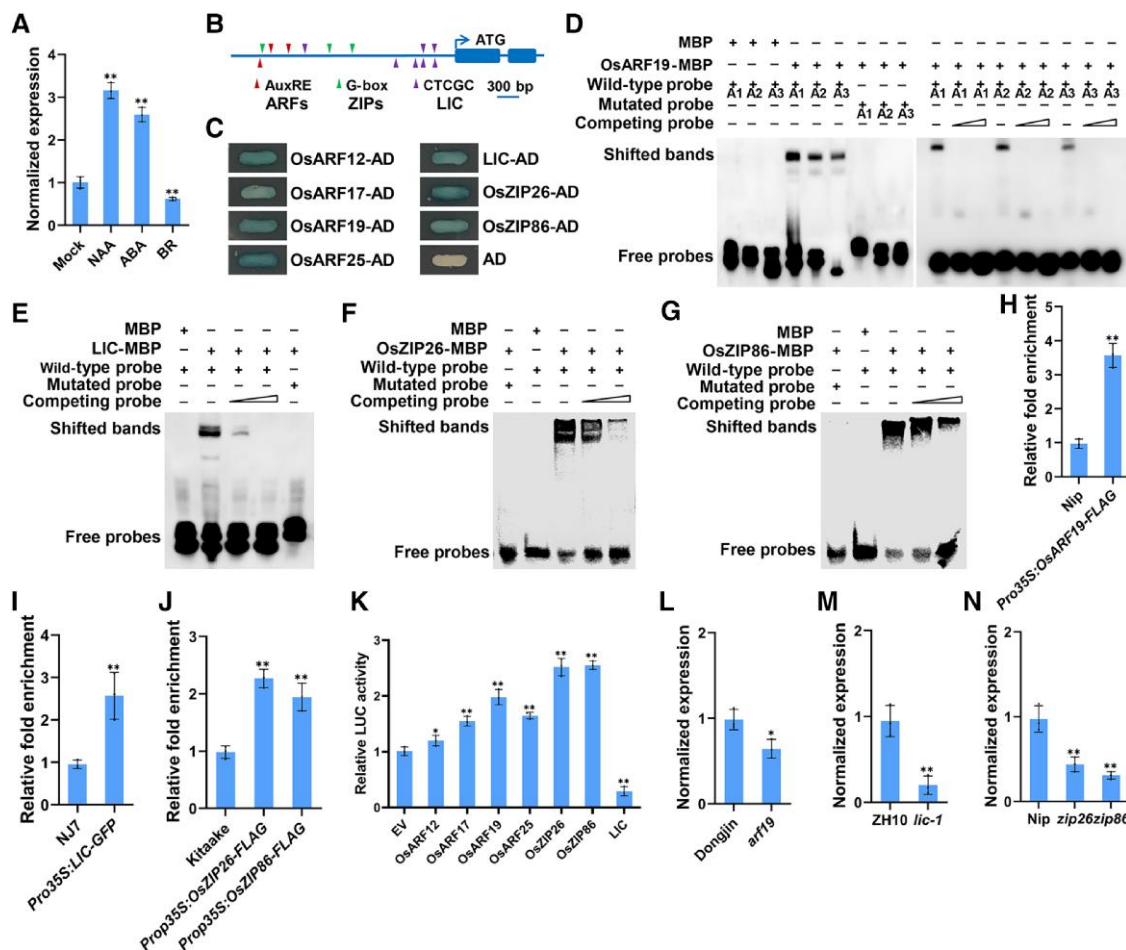


Figure 5. *OsSH11* integrates multiple hormone signaling pathways. **A)** Transcript levels of *OsSH11* in WT plants treated with 1 μ M NAA, BR, or ABA for 1 h ($n = 3$). *UBIQUITIN* gene was used as the endogenous control, and relative expression levels were normalized to *UBIQUITIN* which was set as 1. **B)** Schematic depiction of the diverse *cis*-elements of multiple hormone pathways within the 2.5-kb promoter region of *OsSH11*. The recognition motifs of corresponding transcription factors are shown below. The arrow indicates the transcriptional start site. The amplified region for CHIP-qPCR analysis is marked by the yellow line. A1 to A3, AuxRE1-AuxRE3; G1 to G3, G-box1-G-box 3. **C)** Y1H screening assay shows that multiple upstream transcription factors can bind to the promoter region of *OsSH11*. The empty pB42AD vector (AD) was used as the negative control. **D to G)** EMSA validates that OsARF19 **D)**, LIC **E)**, OsZIP26 **F)**, and OsZIP86 **G)** bind directly to the corresponding motifs in the promoter of *OsSH11*. MBP protein was used as the negative control. – and + indicate the absence and presence of the corresponding proteins or probes. The triangles indicate increased amounts of competing probes. A1 to A3 represent AuxRE1-AuxRE3 in **D)**. **H to J)** ChIP-qPCR analysis verifies the enrichment of OsARF19, LIC, OsZIP26 and OsZIP86 to the promoter region of *OsSH11* in vivo ($n = 3$). The fold enrichment was calculated as IP/Input. **K)** LUC assay determining the effect of the upstream transcription factors on the expression of *OsSH11* in rice protoplasts. Relative LUC activity was calculated by LUC/Ren and normalized to that of empty vector (EV) control which was set as 1 ($n = 3$). **L to N)** Expression levels of *OsSH11* in the *arf19*, *lic-1*, *zip26*, and *zip86* mutant plants ($n = 3$). *UBIQUITIN* gene was used as the endogenous control, and relative expression levels were normalized to *UBIQUITIN* which was set as 1. Values are means \pm SD, and the statistically significant differences were determined by Students *t*-test (* $P < 0.05$ and ** $P < 0.01$) in **A)** and **H to N)**.

OsZIP26 and OsZIP86 are 2 evolutionarily close bZIP transcription factors in rice with conserved DNA-binding domains (Supplemental Fig. S13D). RT-qPCR analysis showed that OsZIP26 and OsZIP86 were constitutively expressed in various tissues with similar expression patterns, and both of them could be induced by ABA treatment (Supplemental Fig. S13, E to G). OsZIP26 and OsZIP86 proteins localized specifically in the nucleus and form homodimers and heterodimers with each other in the epidermal cells of *Nicotiana benthamiana* leaves (Supplemental Fig.

S13, H and I). In addition, previous studies suggest that LIC acts as a negative regulator of BR signaling and is induced by BR (Zhang et al. 2012).

To verify that these transcription factors directly regulate *OsSH11* expression in planta, we performed transient expression assays with rice protoplasts. The results showed that OsARF12, OsARF17, OsARF25, and especially OsARF19 could significantly activate transcription of *OsSH11* in rice protoplasts (Fig. 5K). Similarly, OsZIP26 and OsZIP86 also activated the transcription of *OsSH11*, whereas LIC repressed the

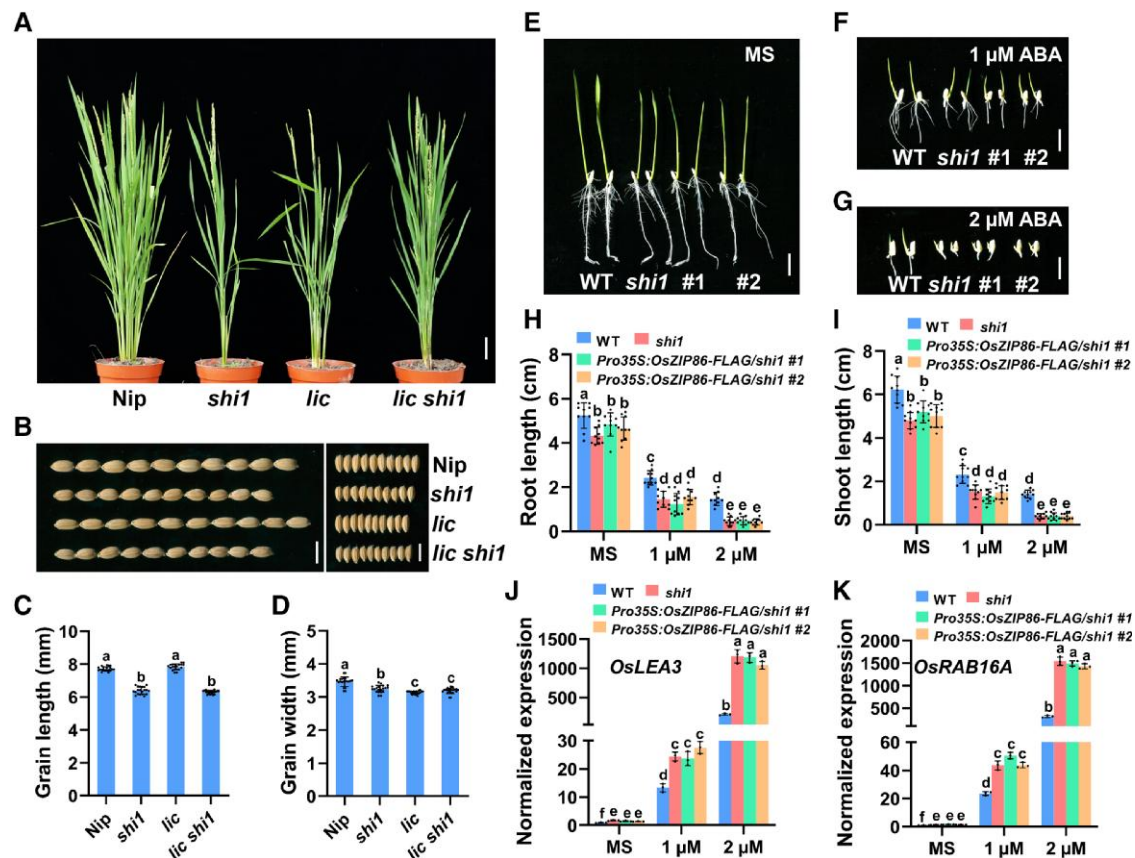


Figure 6. *LIC* and *OsZIP86* act upstream of *OsSHI1*. **A, B**) Plant architecture **A**) and grain size **B**) of *Nip*, *shi1*, *lic*, and *lic shi1* mutants. Bars = 10 cm in **A**) and 8 mm in **B**). **C, D**) Grain length **C**) and width **D**) of *Nip*, *shi1*, *lic*, and *lic shi1* mutants ($n = 20$ grains). **E to I**) Growth phenotypes of WT, *shi1*, and *Pro35S:OsZIP86-FLAG/shi1* transgenic plants treated with 0 (MS) **E**), 1 ABA **F**), and 2 μ M ABA **G**) for 5 d ($n = 10$ plants). Bars = 1 cm. #1 and #2 represent the 2 independent *Pro35S:OsZIP86-FLAG/shi1* transgenic lines. **J, K**) Expression levels of *OsLEA3* **J**) and *OsRAB16A* **K**) in WT, *shi1*, and *Pro35S:OsZIP86-FLAG/shi1* transgenic plants treated with 0 (MS), 1 ABA, and 2 μ M ABA for 5 d ($n = 3$). *UBIQUITIN* gene was used as the endogenous control, and relative expression levels were normalized to *UBIQUITIN* which was set as 1. Values are means \pm SD, and the statistically significant differences were determined by 2-way ANOVA in **C, D**), and **H to K**).

expression of *OsSHI1* (Fig. 5K). Consistent with these findings, RT-qPCR analyses revealed that the expression level of *OsSHI1* was significantly compromised in the *arf19* mutant (Zhang et al. 2016b), *zip26* and *zip86* loss-of-function mutants (generated with the CRISPR/Cas9 technology), and the *lic-1* gain-of-function mutant (Zhang et al. 2012) (Fig. 5, L to N). Moreover, we found that the *arf19* mutant had reduced lateral roots, similar to *shi1* (Supplemental Fig. S14, A and B) and that auxin-induced *OsSHI1* transcription was evidently reduced in *arf19* (Supplemental Fig. S14C). As expected, drought tolerance was obviously enhanced in the *zip26* and *zip86* mutants (Supplemental Fig. S15, A to F), and consistently, seed germination and growth of the *zip26* and *zip86* mutant plants were more sensitive to ABA treatment (Supplemental Fig. S15, G to P), similar to the *shi1* mutant.

Intriguingly, we also found 1 *OsSHI1* recognition motif (ACTCTAC) in the promoter of *OsSHI1* (Supplemental Figs. S9 and S16A). Y1H and EMSA validated that *OsSHI1* directly bound to its own promoter through the ACTCTAC motif (Supplemental Fig. S16, B and C). Further transient

expression assay showed that *OsSHI1* suppressed its own transcription in rice protoplasts (Supplemental Fig. S16D). Together, these observations suggest that *OsSHI1* is subject to negative feedback regulation by itself.

OsSHI1 acts downstream of *LIC*, *OsARF19*, and *OsZIP26/86*

To further confirm the role of *LIC*, *OsARF19*, *OsbZIP26*, and *OsZIP86* in regulating plant architecture and stress responses through mediating *OsSHI1* expression, we generated and characterized the phenotype of *Pro35S:LIC-GFP*, *Pro35S:OsARF19-FLAG*, *Pro35S:OsZIP26-FLAG*, and *Pro35S:OsZIP86-FLAG* transgenic plants. As expected, the *Pro35S:LIC-GFP* transgenic plants displayed a BR-defective phenotype (such as compact plant, shortened, and widened grains) (Supplemental Fig. S17, A to D), whereas the *Pro35S:OsARF19-FLAG* transgenic plants displayed a BR- and auxin-enhanced phenotype (such as loose plant architecture, lengthened, and narrowed grains as well as increased lateral

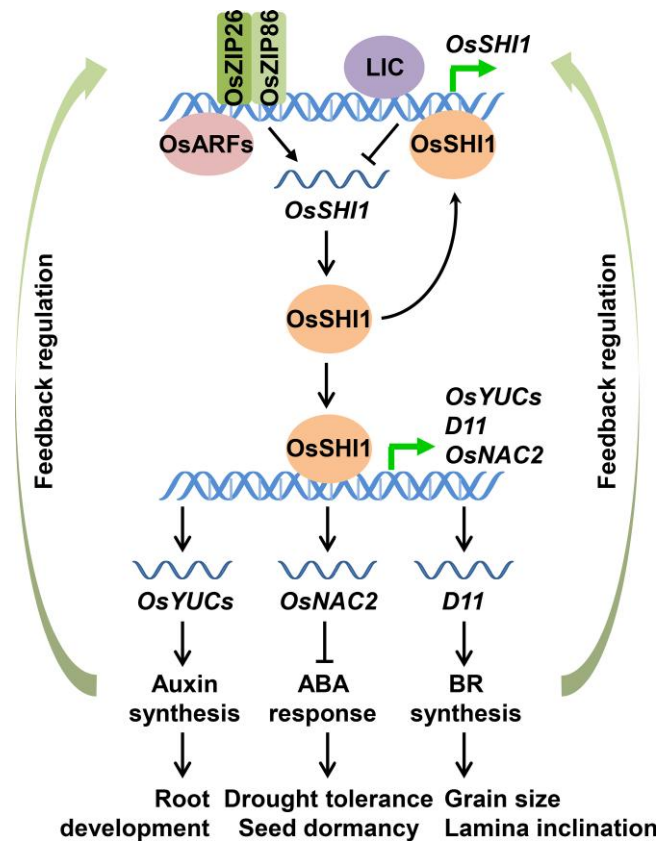


Figure 7. A schematic model of integration of auxin, BR, and ABA hormone pathways by *OsSHI1*. *OsARFs*, *OsZIP26/86*, and *LIC*, upstream transcription factors of auxin, ABA, and BR pathways, converge on the promoter region of *OsSHI1* to activate or repress its transcription, respectively. The *OsSHI1* protein then binds directly to the promoters of *OsYUCs*, *D11*, and *OsNAC2* to participate in the biosynthesis of auxin, BR, and signaling of ABA to modulate plant growth and adaptation. In return, auxin, BR, and ABA induce the transcriptions of *OsARFs*, *LIC*, and *OsZIP26/86*. Besides, *OsSHI1* is subject to negative feedback regulation by itself.

root number) (Supplemental Fig. S17, E to J). The expression levels of *LIC* and *OsARF19* were significantly increased in *Pro35S:LIC-GFP* and *Pro35S:OsARF19-FLAG* transgenic plants, respectively (Supplemental Fig. S17, K and L). Moreover, the expression level of *OsSHI1* was evidently upregulated in the *Pro35S:OsARF19-FLAG* transgenic plants (Supplemental Fig. S17M). In addition, the *ProUbi:OsSHI1* transgenic plants also displayed auxin-enhanced root growth (Supplemental Fig. S1, A to D). Moreover, the *Pro35S:OsZIP26-FLAG* and *Pro35S:OsZIP86-FLAG* transgenic plants displayed an expected ABA-deficient phenotype (such as reduced drought tolerance and ABA sensitivity) (Supplemental Fig. S18), in contrast to the *shi1*, *zip26*, and *zip86* mutants.

To verify the genetic relationship between *OsSHI1* with *LIC*, *OsZIP26*, and *OsZIP86*, we generated the *lic* and *lic shi1* mutants using the CRISPR/Cas9 technology in Nip background as well as the *Pro35S:OsZIP86-FLAG* transgenic plant in the *shi1* background, respectively (Supplemental Fig. S19).

Compared with Nip, the *lic* single mutant exhibited a BR-enhanced phenotype with slightly increased leaf inclination and significantly more slender grain size. However, the *lic shi1* double mutant displayed similar BR-deficient morphologies to *shi1* (such as compact plant architecture and smaller grain) (Fig. 6, A to D). Besides, in contrast to the ABA hyposensitivity of the *Pro35S:OsZIP86-FLAG* transgenic plant (Supplemental Fig. S18), the *Pro35S:OsZIP86-FLAG/shi1* transgenic plant was still hypersensitive to ABA (Fig. 6, E to K), similar to the *shi1* mutant. Taken together, these genetic results demonstrated that *OsSHI1* acts downstream of *OsARF19*, *LIC*, *OsZIP26*, and *OsZIP86* to mediate the signaling integration of auxin, BR, and ABA, thus orchestrating plant growth and stress adaptation in rice.

Discussion

The sophisticated plasticity of plant development and adaptation largely relies on cross talk of interconnected hormonal signaling pathways to coordinate cellular activities and developmental processes. In this study, we demonstrate that *OsSHI1* acts as an essential transcriptional hub that integrates the signaling pathways of auxin, BR, and ABA, to balance the growth and stress adaptation in rice (Fig. 7).

SHI transcription factors are involved in multiple hormone pathways

The *SHI* gene family encodes plant-specific transcription factors with diverse biological functions for leaf and flower specification and photomorphogenesis in *Arabidopsis*, awn, and inflorescence patterning in barley (*Hordeum vulgare*) as well as tillering and panicle size in rice (Kuusk et al. 2006; Yuo et al. 2012; Youssef et al. 2017; Yuan et al. 2018; Duan et al. 2019). Several studies revealed that some phenotypic variations caused by malfunction of *SHI* genes are likely mediated through various hormone signaling pathways. For instance, *STYLISH1* (*STY1*, a *SHI* homolog) genetically interacts with auxin transport/signaling factors, such as *PIN-FORMED1* (*PIN1*), *PINOID* (*PID*), and *ETTIN* (*ETT*) during gynoecia development in *Arabidopsis* (Sohlberg et al. 2006). Besides, the dwarfism of *Arabidopsis shi* mutant may be associated with defect in gibberellic acid (GA) biosynthesis, indicating that *SHI* is a potential suppressor of GA responses (Fridborg et al. 1999, 2001). *VRS2* (*six-rowed spike 2*), a *SHI* family gene in barley, affects auxin, cytokinin (CK), and GA homeostasis and gradients as well as sucrose metabolism during inflorescence and shoot patterning (Youssef et al. 2017). *GRMZM2G077752*, 1 of the *SHI-RELATED SEQUENCE* (*SRS*) genes in maize (*Zea mays*), coexpresses with genes involving in ABA signaling and carbohydrate remobilization during leaf senescence (He et al. 2020).

In this study, we provided detailed phenotypic, molecular, and genetic evidences to demonstrate that *OsSHI1* mediates the transcriptional interplay between auxin, BR, and ABA to balance the growth and stress adaptation in rice (Fig. 7),

deepening our understanding into the detailed roles of *SHI* genes in the regulation of hormone-mediated plant developmental processes. However, the participation and regulatory mechanisms of SHI transcription factors in other hormone pathways (such as strigolactones, jasmonic acid, salicylic acid, and ethylene) and in response to environmental factors (such as light, temperature, salinity, and biotic stress) remain to be further elucidated.

OsSHI1 is a key transcriptional hub for auxin, BR and ABA

Previous studies have discovered that the antagonism between auxin, ABA, and BR signaling pathways mainly entails protein–protein interaction and posttranslational modifications of key components of each signaling pathway. For example, dephosphorylation of BRASSINOSTEROID INSENSITIVE2 (BIN2) by Protein Phosphatase 2Cs (PP2Cs), ABA INSENSITIVE 1 (ABI1), and ABI2 dampens the activity of BIN2, a key kinase which can activate/stabilize Snf-related kinase 2 (SnRK2) and ABI5 transcription factor to regulate plant growth and adaptation to stress (Cai et al. 2014; Wang, Tang, et al. 2018). The Remorin family protein OsREM4.1, which is transcriptionally upregulated by ABA, hinders the formation and activation of OsBRI1 (BR INSENSITIVE 1)-OsSERK1 (SOMATIC EMBRYOGENESIS RECEPTOR KINASE 1) complex and represses BR signaling initiation (Gui et al. 2016). BES1 (BR INSENSITIVE1 EMS SUPPRESSOR1) interacts and interferes the transcriptional activity of ABI5 to suppress ABA signaling output (Zhao et al. 2019). BIN2-mediated phosphorylation of ARF2, ARF7, and ARF19 potentiates auxin response during lateral root development (Vert et al. 2008; Cho et al. 2014).

In this study, we show that loss-of-function mutation in *OsSHI1* leads to a pleiotropic phenotype related to deficiencies in auxin, BR, and ABA hormone signaling processes. The repressed root growth of *shi1* is likely caused by weakened auxin signaling; compact plant architecture and reduced grain size are likely caused by dampened BR signaling, whereas enhanced seed dormancy and drought tolerance are likely caused by enhanced ABA signaling (Figs. 1, 2, and S1S2). In addition, we show that several direct upstream transcription factors, such as OsARFs, OsZIP26/86, and LIC, converge on the promoter region of *OsSHI1* to active or inhibit its transcription (Fig. 5). OsARFs (OsARF12, OsARF17, OsARF25, and especially OsARF19) likely mediate auxin-induced transcriptional activation of *OsSHI1*, whereas OsZIP26 and OsZIP86 likely mediate ABA-induced transcriptional activation of *OsSHI1*, and LIC likely mediates BR-repression of *OsSHI1* expression (Fig. 5).

Moreover, OsSHI1 then promotes the biosynthesis of auxin and BR by directly activating the expression of *OsYUCCA*s and *D11* but represses the signaling of ABA by directly activating the expression of *OsNAC2* to coordinate plant growth and stress adaptation (Fig. 3). In turn, auxin, BR, and ABA induce the transcription of *OsARFs*, *LIC*, and *OsZIP26/86*,

respectively (Supplemental Fig. S13, C and G; Zhang et al. 2012). Therefore, the expression of *OsSHI1* is subjected to positive feedback regulation by auxin and ABA signaling but negative feedback regulation by BR signaling. Notably, *OsSHI1* can also bind to its own promoter and suppress its own expression (Supplemental Fig. S16). Together, our results demonstrate that *OsSHI1* is a key transcriptional hub that orchestrates the coordination of the signaling pathways of growth-promoting hormones (auxin and BR) and stress hormone (ABA) to fine-tune the balance of growth and stress adaptation in rice, thus providing insight into signaling integration and feedback regulation of auxin, BR, and ABA at the transcriptional level by a versatile transcription factor in plants (Fig. 7).

Potential utilization of *OsSHI1* to improve yield and stress adaptation

Breeding high-yielding, yet environmental stress-resilient crops holds significant promise in face of the fluctuating climate changes and increasing human population. We previously reported that mutation in *OsSHI1* confers a typical ideal plant architecture characterized with reduced tiller number, strong culm, and enlarged panicle (Duan et al. 2019). In this study, we further show that the *shi1* mutant possesses enhanced stress resilience (Fig. 1, J to O). These features are desirable for breeding high-yielding and stress-resilient rice cultivars. However, mutation in *OsSHI1* is also associated with several detrimental defects, such as reduced seed setting rate (Duan et al. 2019) and grain size (Fig. 11). Therefore, fine-tuning of the expression levels and detailed dissection of the regulatory mechanisms of *OsSHI1* and *SHI-like* genes in other crops may provide strategies to uncouple the favorable and unfavorable effects of *OsSHI1* on agronomic traits for simultaneous improvement of yield and stress adaptation in rice and other crops.

Materials and methods

Plant materials and growth conditions

The rice (*O. sativa* L.) *shi1*, *d11-2*, *lic-1*, and *arf19* mutants were described in previous studies (Tong et al. 2012; Zhang et al. 2012; Zhang et al. 2016b; Duan et al. 2019). *OsSHI1*-CRISPR (*shi1*), *D11*-CRISPR (*d11*), *D11/OsSHI1*-CRISPR (*d11 shi1*), *OsNAC2*-CRISPR (*nac2*), *OsNAC2/OsSHI1*-CRISPR (*nac2 shi1*), *LIC*-CRISPR (*lic*), *LIC/OsSHI1*-CRISPR (*lic shi1*), *OsZIP26*-CRISPR (*zip26*), *OsZIP86*-CRISPR (*zip86*), *ProUbi:OsSHI1*, and *Pro35S:OsARF19-FLAG* transgenic plants were generated in the Nip background. *ProUbi:OsSHI1* transgenic plants were also generated in the ZH11 and *d11-2* backgrounds. *Pro35S:LIC-GFP* and *OsYUCCA1*-CRISPR (*yucca1*) transgenic plants were generated in the Ningjing7 (NJ7) background. *Pro35S:OsZIP26-FLAG* and *Pro35S:OsZIP86-FLAG* transgenic plants were generated in the Kitaake (Kit) or *shi1* background. Plants were grown in the paddy field at Nanjing Agricultural University (Nanjing, China) under natural conditions with conventional management.

All the rice materials used for detecting the hormone responses and germination rates were grown in a growth chamber with a 14.5-/9.5-h light/dark cycle at 30 °C/25 °C. Light was provided by white light-emitting diode (LED) tubes (400 to 700 nm, 250 $\mu\text{mol m}^{-2} \text{s}^{-1}$). *N. benthamiana* plants were grown under a 16-/8-h light/dark cycle (150 $\mu\text{mol m}^{-2} \text{s}^{-1}$) at 22 °C (50% humidity), and 5-wk-old leaves were used for transient expression experiments.

Endogenous hormone content measurement

Approximately 2-g (fresh weight) tissues of WT and *shi1* young plants were collected and ground into fine powder in liquid nitrogen. The contents of IAA, TY, CS, and ABA were measured using the HPLC separation coupled with ion trap MS employing ESI method (ESI-HPLC-MS) (Fu et al. 2012; Xin et al. 2013).

Hormone, gravitropic, and drought response determination

Ten-day-old plants of WT and *shi1* were grown in one-half-strength MS (Phytotech, M524) hydroponic culture medium supplemented with 1 μM NAA (Phytotech, N600), ABA (Phytotech, A102), and BR (Sigma, E1641). The identical volume of solvent was used as the mock treatment. One hour after hormone treatment, the shoot tissues were taken to identify the responses of *OsSHI1* to different hormones. The lamina joint inclination was measured at 12-h intervals after hormone treatment using ImageJ software (Tian et al. 2017).

For seed germination and growth assay, husked seeds were surface sterilized with 70% (*v/v*) ethanol for 1 min and washed twice with sterilized water. Then, the seeds were immersed in 10% NaClO solution for 30 min, intensively rinsed with sterilized water and planted onto half-strength MS medium supplemented with 0.4% Gelzan (Sino Industrial, G3251) and gradient concentration of NAA or ABA (0, 1, and 2 μM). Seed germination was defined as the emergence of coleoptile of 5 mm in length, and germinated seeds were counted at 12-h intervals after hormone treatment. Root and shoot growth of plants were measured and photographed on the fifth day.

To investigate the gravitropic responses, plants were grown vertically on half-strength MS medium for 3 d and then rotated 90° to allow growing for another 1 h. The root and shoot curvatures were measured using ImageJ software.

Drought treatment was performed according to the previously published method (Ning et al. 2011) with some modifications. Briefly, germinated seeds of different genotypes were planted in the same container with identical intervals and proper moisture. Drought-induced phenotypes of treated plants were observed after withholding water for the indicated time period. After recovery from rehydration, the survival rates of drought-treated plants were recorded.

RT-qPCR analysis

Total RNA of different tissues or genotypes was extracted using the ZR Plant RNA MiniPrep Kit (Zymo research, R2024) according to the manufacturer's recommendations. The first-strand cDNA was synthesized based on the QuantiTect Reverse Transcription Kit (Qiagen, 205311). RT-qPCR was performed on the CFX96 Real-Time System (BIO-RAD) using SYBR Premix Ex Taq (Takara, RR820) with the rice *UBIQUITIN* gene as the endogenous control. Relative gene expression levels were quantitated based on 3 biological replicates via the $2^{-\Delta\Delta Ct}$ method (Livak and Schmittgen 2001). All primer pairs used for RT-qPCR analysis are listed in Supplemental Table S1.

Vectors construction and plant transformation

For genome-editing of *OsSHI1*, *OsNAC2*, *D11*, *OsZIP26*, *OsZIP86*, *LIC*, and *OsYUCCA1*, 20-bp gene-specific target sequences were selected by the target-designing website (<http://crispr.hzau.edu.cn/cgi-bin/CRISPR/CRISPR>) and inserted into the *AarI* restriction site of the TKC plasmid (He et al. 2018). The generated constructs were subsequently introduced into the calli of Nip or NJ7 via *Agrobacterium tumefaciens*-mediated transformation (Hiei et al. 1994), and the positive transgenic plants were identified by sequencing.

To generate the GFP/FLAG tag-fused proteins in vivo, the full-length coding regions of *LIC*, *OsZIP26*, *OsZIP86*, and *OsARF19* were amplified and inserted into the *XbaI* restriction site of the pCAMBIA1305-GFP or 1300-221-3 \times FLAG binary vectors (Ren et al. 2014). The generated constructs were then introduced into the calli of NJ7, Kit, or Nip via *Agrobacterium*-mediated transformation (Hiei et al. 1994). All primer pairs used for vector constructions are listed in Supplemental Table S2.

Y1H assay

Y1H analysis was performed according to the previously described method (Lin et al. 2007). Briefly, full-length coding regions of *OsSHI1*, *OsARF12*, *OsARF17*, *OsARF19*, *OsARF25*, *OsZIP26*, *OsZIP86*, and *LIC* were amplified and fused into the *EcoRI* restriction site of the pB42AD vector (Primer pairs listed in Supplemental Table S2). About 2-kb native or mutated (recognition motifs mutated into adenines) promoter regions of *OsYUCCA1*, *OsYUCCA2*, *OsYUCCA4*, *OsYUCCA5*, *OsYUCCA6*, *OsYUCCA7*, *D11*, *OsNAC2*, *OsSHI1*, *OsABA1-4*, and *OsNCED1-5* upstream of the ATG starting codon were cloned into the *XhoI* restriction site of the pLacZi reporter vector (Primer pairs listed in Supplemental Table S2). Various combined constructs were then cotransformed into the yeast (*S. cerevisiae*) strain EGY48. Transformants were grown on SD-Trp/-Ura plates for 3 d at 30 °C and then transferred onto X-gal (5-bromo-4-chloro-3-indolyl- β -d-galactopyranoside, 200 nM) (Sigma, V900468) plates for blue color development. The β -galactosidase activity of the *LacZ* reporter gene was determined using CPRG (Roche, 10884308001) as the

substrate. Detailed procedures were performed according to the manufacturer's recommendations (Clontech).

ChIP analysis

Detailed procedures for ChIP assays were performed according to the previously reported method (Duan et al. 2019). Briefly, ~4-g plants of different genotypes were grounded into fine powder and cross-linked with formaldehyde. The nucleus was then precipitated and the chromatin was sonicated to 200 to 500 bp in length. Protein/DNA complexes were immunoprecipitated with anti-OsSHI1 specific polyclonal antibodies (Duan et al. 2019) or anti-GFP/FLAG Magnetic agaroses (MBL, D153-11/M185-10R). The enriched DNA was used as template for qPCR, and the fold enrichment was calculated as the ratio of IP to Input. All primer pairs were listed in Supplemental Table S1.

Protein induction and purification

Full-length coding regions of *OsSHI1*, *OsARF12*, *OsARF17*, *OsARF19*, *OsARF25*, *OsZIP26*, *OsZIP86*, and *LIC* were fused into the *EcoRI/PstI* or *EcoRI/SalI* restriction sites of the pMAL-c2x expression vector (primer pairs listed in Supplemental Table S2) and transformed into the *Escherichia coli* BL21 (DE3) competent cells (TransGen, CD601). The bacteria were cultured at 37 °C with 200 × g rotation until the optical density (OD) reached ~0.6. Expression of MBP and MBP-tag fusion proteins was induced by 0.4 mM IPTG (isopropyl-β-D-thiogalactoside, Amresco, 0487) at 18 °C for 16 h with gentle shaking (100 × g). The bacteria were collected by centrifugation and the fusion proteins were purified using the Amylose Resin (NEB, E8035S) according to the manufacturer's protocols.

EMSA

3'-DIG-labeled oligonucleotides containing the putative binding sites of *OsSHI1*, *OsARF12*, *OsARF17*, *OsARF19*, *OsARF25*, *OsZIP26*, *OsZIP86*, and *LIC* were synthesized by Invitrogen (Shanghai, China) (probes listed in Supplemental Table S3). EMSAs were carried out using the DIG Gel Shift Kit (Roche, 03353591910) according to the manufacturer's recommendations. Briefly, equal amount of complementary oligonucleotides was denatured at 95 °C for 10 min, slowly cooled down to 15 °C and diluted to 100 fmol/μL concentrations. A total of 100 ng purified proteins were mixed with 100-fmol probes and 2-μg poly(dI-dC) and incubated at room temperature for 30 min. Samples were then subjected to the native polyacrylamide gel (6.5%) in 0.5× TBE buffer (45 mM Tris, 45 mM Boric acid, and 1 mM EDTA). Probes were electro-blotted onto nylon membrane (Roche, 11417240001) at 400 mA for 30 min and immediately cross-linked with UV light for 5 min. The membrane was then incubated in the blocking solution and DIG antibody solution, each for 30 min. After intensive wash, the CSPD working solution was applied to the membrane to visualize the signal by a low-light cooled CCD imaging apparatus (Tanon 5200).

LUC activity determination

About 2-kb promoter regions of *OsYUCCA1*, *OsYUCCA2*, *OsYUCCA4*, *OsYUCCA5*, *OsYUCCA6*, *OsYUCCA7*, *D11*, *OsNAC2*, and *OsSHI1* upstream of the ATG starting codon were cloned into the *NcoI* restriction site upstream of *LUC* reporter gene of the pGreen0800-LUC vector (Chen et al. 2008) to generate the *pOsYUCCA1:LUC*, *pOsYUCCA2:LUC*, *pOsYUCCA4:LUC*, *pOsYUCCA5:LUC*, *pOsYUCCA6:LUC*, *pOsYUCCA7:LUC*, *pD11:LUC*, *pOsNAC2:LUC*, and *pOsSHI1:LUC* reporter constructs (primer pair listed in Supplemental Table S2). Full-length coding regions of *OsARF12*, *OsARF17*, *OsARF19*, *OsARF25*, *OsZIP26*, *OsZIP86*, *LIC*, and *OsSHI1* were inserted into the *BamHI* restriction site of the pAN580 transient vector (Zhang et al. 2016a) to generate the *p35S:OsARF12-GFP*, *p35S:OsARF17-GFP*, *p35S:OsARF19-GFP*, *p35S:OsARF25-GFP*, *p35S:OsZIP26-GFP*, *p35S:OsZIP86-GFP*, *p35S:LIC-GFP*, and *p35S:OsSHI1-GFP* effector constructs, respectively (primer pairs listed in Supplemental Table S2). Five micrograms of the combined reporter and effector plasmids were then cotransformed into the rice protoplasts according to the previously described method (Zhang et al. 2011). The *LUC* gene from *Renilla reniformis* (*Ren*) under the control of CaMV35S promoter was used as the internal control. *LUC* activities were determined by the Dual-luciferase Assay Kit (Promega, E1910) following the manufacturer's recommendations, and the relative *LUC* activity was calculated as the ratio of *LUC*/*Ren*.

Immunoblot analysis

Young plants of different genotypes were grounded into fine powder in liquid nitrogen. Samples were suspended in 2× volumes of Protein Extraction Buffer (50 mM Tris-HCl pH 8.0, 150 mM NaCl, 10 mM MgCl₂, 1 mM EDTA, 10% [v/v] glycerol, and 1× protease inhibitor cocktail) and incubated at 4 °C for 30 min with gentle rotation. After centrifuging at 12,000 × g for 10 min at 4 °C, the supernatant was boiled in 1× protein loading buffer (50 mM Tris-HCl pH 6.8, 2% SDS, 0.1% bromophenol blue, 10% glycerol, and 1% β-mercaptoethanol) at 100 °C for 10 min. Protein samples were then separated by 10% SDS-PAGE gel, transferred to Immobilon PVDF membrane (Millipore, IPVH00010), and immunoblotted with anti-OsSHI1-specific polyclonal antibodies (Duan et al. 2019) or anti-HSP antibody (Beijing Protein Innovation, AbM51099-31-PU) at 1:2,000 and 1:10,000 dilutions, respectively. Signals were visualized with Chemistar High-sig ECL Western Blotting Substrate (Tanon, 180-501) by a low-light cooled CCD imaging apparatus (Tanon 5200).

Firefly LUC complementation assay

Full-length coding regions of *OsZIP26* and *OsZIP86* were amplified (primer pairs listed in Supplemental Table S2) and inserted into the *BamHI/SalI* restriction sites of the pCAMBIA-nLUC vector or the *KpnI/SalI* restriction sites of the pCAMBIA-cLUC vector, respectively. The combined nLUC and cLUC constructs were cointroduced into leaves of 5-wk-old *N. benthamiana* plants through *Agrobacterium*

leaf infiltration. Three days after infiltration, detached leaves were sprayed with 1 mM luciferin reagent (Solarbio, D9390) and incubated in darkness for 5 min before LUC image taking using a low-light cooled CCD imaging apparatus (Tanon 5200).

Subcellular localization

The full-length coding regions of *OsZIP26* and *OsZIP86* were fused into the *Xba*I restriction site upstream of GFP (green fluorescent protein) in the pCAMBIA1305-GFP binary vector driven by the double CaMV35S promoter (primer pairs listed in [Supplemental Table S2](#)). The generated *Pro35S::OsZIP26-GFP* and *Pro35S::OsZIP86-GFP* constructs were introduced into the *A. tumefaciens* strain EHA105 and then coinfiltrated with the p19 strain into leaves of 5-wk-old *N. benthamiana* plants. Two days after infiltration, the fluorescence signals of GFP in epidermal cells were observed by the confocal laser scanning microscope (Leica SP8). GFP was excited at 488 nm, and the emission was detected at 500 to 550 nm.

Phylogenetic analysis

The accession numbers and full-length coding regions of *AtARFs*, *OsARFs*, and *OsZIPs* were previously reported ([Wang et al. 2007](#); [Zg et al. 2014](#)) and obtained from the NCBI database (<https://www.ncbi.nlm.nih.gov/gene/>). Multiple sequence alignments of these proteins were performed using the ClustalW program ([Supplemental Files 1 and 2](#)). The phylogenetic tree was constructed using the maximum likelihood method using the MEGA 7 software with 1,000 bootstrap replications ([Kumar et al. 2016](#)).

Quantification and statistical analysis

All plant materials used for phenotype identification, hormone measurement or treatment, and RT/ChIP-qPCR analyses were grown simultaneously in the same conditions and time period with identical management. The statistical graphs were generated and processed by the GraphPad Prism 8 software. All values are presented as means \pm SD, and the statistically significant differences between the control and experimental groups were determined by 2-sided Student's *t*-test ($*P < 0.05$ and $**P < 0.01$) or 2-way ANOVA. The exact numbers of samples and replicates are indicated in the legends. Detailed descriptions of controls, quantifications, and statistical analyses can be found in the figure legends. No data were excluded from analyses. All the analyzed results are displayed in [Supplemental Data Set 1](#).

Accession numbers

Genome sequence data from this study can be found in the GenBank/EMBL libraries under the following accession numbers: Os09g0531600 (*OsSHI1*), Os01g0645400 (*OsYUCCA1*), Os05g0528600 (*OsYUCCA2*), Os01g0224700 (*OsYUCCA4*), Os12g0512000 (*OsYUCCA5*), Os07g0437000 (*OsYUCCA6*), Os04g0128900 (*OsYUCCA7*), Os04g0469800 (*D11*), Os04g0460600 (*OsNAC2*), Os04g0671900 (*OsARF12*),

Os06g0677800 (*OsARF17*), Os06g0702600 (*OsARF19*), Os12g0613700 (*OsARF25*), Os06g0704300 (*LIC*), Os03g0239400 (*OsZIP26*), Os12g0233800 (*OsZIP86*), Os04g0448900 (*OsABA1*), Os03g0810800 (*OsABA2*), LOC_Os06g45860 (*OsABA3*), Os01g0128300 (*OsABA4*), Os02g0704000 (*OsNCED1*), Os12g0435200 (*OsNCED2*), Os03g0645900 (*OsNCED3*), Os07g0154100 (*OsNCED4*), Os12g0617400 (*OsNCED5*), and Os03g0234200 (*Ubiquitin*).

Acknowledgments

We thank Chengcai Chu for providing the *d11-2* seed. We thank Kang Chong for providing the *lic-1* seed.

Author contributions

E.D., L.J., H.W., and J.W. designed the research. E.D., Q.L., Y.H.W., Y.R., H.X., Y.Z., Y.L.W., X.T., H.D., Y.P.W., X.J., X.C., J.L., H.Y., and R.C. performed the experiments. E.D., Q.L., Y.H.W., Y.R., H.X., Y.Z., Y.L.W., X.T., H.D., Y.P.W., X.J., X.C., J.L., H.Y., and R.C. analyzed data. E.D., Q.L., H.W., and J.W. wrote the paper. All authors read and approved the final article.

Supplemental data

The following materials are available in the online version of this article.

Supplemental Figure S1. Phenotypes of Nip and its *ProUbi::OsSHI1* transgenic plants.

Supplemental Figure S2. Responses of Nip and the *ProUbi::OsSHI1* transgenic plants to NAA, BR, and ABA treatment.

Supplemental Figure S3. *OsSHI1* indirectly regulates ABA biosynthesis.

Supplemental Figure S4. Schematic depictions of the *cis*-elements in the promoter regions of *OsYUCCAs*, *D11*, and *OsNAC2*.

Supplemental Figure S5. β -Galactosidase activities of the *LacZ* reporter gene driven by promoters of *OsSHI1*'s target genes in Y1H assays.

Supplemental Figure S6. Negative control of MBP protein in the EMSA analyses for *OsYUCCAs*.

Supplemental Figure S7. *OsSHI1* functions upstream of *D11* and *OsNAC2*.

Supplemental Figure S8. Root phenotype of *yucca1* mutant.

Supplemental Figure S9. Motif characterization in the promoter region of *OsSHI1*.

Supplemental Figure 10. β -Galactosidase activities of the *LacZ* reporter gene driven by *OsSHI1* promoter in Y1H assays.

Supplemental Figure 11. Y1H assay showing the binding of *LIC* to the promoter region of *OsSHI1*.

Supplemental Figure 12. EMSA verifies the direct binding of upstream transcription factors to the corresponding motifs in the promoter region of *OsSHI1*.

Supplemental Figure 13. Characterization of upstream ARF and ZIP transcription factors.

Supplemental Figure S14. Root morphology of the *arf19* mutant.

Supplemental Figure 15. Drought tolerance and ABA responses of Nip and its *zip26* and *zip86* mutants.

Supplemental Figure 16. *OsSHI1* undergoes negative feedback regulation of its own expression.

Supplemental Figure 17. Phenotypes of *Pro35S:LIC-GFP* and *Pro35S:OsARF19-FLAG* transgenic plants.

Supplemental Figure 18. ABA sensitivity of Kit and its *Pro35S:OsZIP26-FLAG* and *Pro35S:OsZIP86-FLAG* transgenic lines.

Supplemental Figure 19. Identification of *lic shi1* and *p35S:OsZIP86-FLAG/shi1* transgenic plants.

Supplemental Table S1. Sequences of primers used for RT/ChIP-qPCR analyses.

Supplemental Table S2. Sequences of primers used for vector constructions.

Supplemental Table S3. Sequences of probes used for EMSA.

Supplemental Data Set 1. Detailed descriptions of statistical analyses.

Supplemental File 1. Text file of the alignment used for the phylogenetic analysis of OsARFs shown in Supplemental Fig. S13A.

Supplemental File 2. Text file of the alignment used for the phylogenetic analysis of OsZIPs shown in Supplemental Fig. S13D.

Funding

This research was supported by grants from the National Natural Science Foundation of China (31901513, 92035301), the Fundamental Research Funds for the Central Universities (KJQN202005), the China Postdoctoral Science Foundation (2019M661864), and the Jiangsu Province Agriculture Independent Innovation Fund Project (CX(19)1002). This work was also supported by the Jiangsu Nanjing National Field Scientific Observation and Research Station for Rice Germplasm Resources and the Jiangsu Engineering Research Center for Plant Genome Editing.

Conflict of interest statement. The authors declare no conflict of interests.

Data availability

All experimental data are available and accessible via the main text and the supplemental data.

References

Achard P, Cheng H, De L, Jan G, Hermien D, Thomas S, Dominique M, Straeten V, Peng J, Harberd N. Integration of plant responses to environmentally activated phytohormonal signals. *Science* 2006;**311**:(5757):91–94. <https://doi.org/10.1126/science.1118642>

Cai Z, Liu J, Wang H, Yang C, Chen Y, Li Y, Pan S, Dong R, Tang G, Barajas-Lopez J, et al. GSK3-like kinases positively modulate abscisic acid signaling through phosphorylating subgroup III SnRK2s in *Arabidopsis*. *Proc Natl Acad Sci*. 2014;**111**(26):9651–9656. <https://doi.org/10.1073/pnas.1316717111>

Chaiwanon J, Wang W, Zhu J, Oh E, Wang Z. Information integration and communication in plant growth regulation. *Cell* 2016;**164**(6):1257–1268. <https://doi.org/10.1016/j.cell.2016.01.044>

Chen H, Zou Y, Shang Y, Lin H, Wang Y, Cai R, Tang X, Zhou J. Firefly luciferase complementation imaging assay for protein–protein interactions in plants. *Plant Physiol*. 2008;**146**(2):323–324. <https://doi.org/10.1104/pp.107.111740>

Cho H, Ryu H, Rho S, Hill K, Smith S, Audenaert D, Park J, Han S, Beeckman T, Bennett M, et al. A secreted peptide acts on BIN2-mediated phosphorylation of ARFs to potentiate auxin response during lateral root development. *Nat Cell Biol*. 2014;**16**(1):66–76. <https://doi.org/10.1038/ncb2893>

Duan E, Wang Y, Li X, Lin Q, Zhang T, Wang Y, Zhou C, Zhang H, Jiang L, Wang J, et al. OsSHI1 regulates plant architecture through modulating the transcriptional activity of IPA1 in rice. *Plant Cell* 2019;**31**(5):1026–1042. <https://doi.org/10.1105/tpc.19.00023>

Fridborg I, Kuusk S, Moritz T, Sundberg E. The *Arabidopsis* dwarf mutant *shi* exhibits reduced gibberellin responses conferred by overexpression of a new putative zinc finger protein. *Plant Cell*. 1999;**11**(6):1019–1032.

Fridborg I, Kuusk S, Robertson M, Sundberg E. The *Arabidopsis* protein SHI represses gibberellin responses in *Arabidopsis* and barley. *Plant Physiol*. 2001;**127**(3):937–948.

Fu J, Chu J, Sun X, Wang J, Yan C. Simple, rapid, and simultaneous assay of multiple carboxyl containing phytohormones in wounded tomatoes by UPLC-MS/MS using single SPE purification and isotope dilution. *Anal Sci*. 2012;**28**(11):1081–1087. <https://doi.org/10.2116/analsci.28.1081>

Fujioka S, Yokota T. Biosynthesis and metabolism of brassinosteroids. *Annu Rev Plant Bio*. 2003;**54**(1):137–164. <https://doi.org/10.1146/annurev.arplant.54.031902.134921>

Gui J, Zhang S, Liu C, Shen J, Li J, Li L. OsREM4.1 interacts with OsSERK1 to coordinate the interlinking between abscisic acid and brassinosteroid signaling in rice. *Dev Cell*. 2016;**38**(2):201–213. <https://doi.org/10.1016/j.devcel.2016.06.011>

He B, Shi P, Lv Y, Gao Z, Chen G. Gene coexpression network analysis reveals the role of SRS genes in senescence leaf of maize (*Zea mays* L.). *J Genet*. 2020;**99**:3.

He Y, Zhu M, Wang L, Wu J, Wang Q, Wang R. Programmed self-elimination of the CRISPR/Cas9 construct greatly accelerates the isolation of edited and transgene-free rice plants. *Mol Plant*. 2018;**11**(9):1210–1213. <https://doi.org/10.1016/j.molp.2018.05.005>

Hiei Y, Ohta S, Komari T, Kumashiro T. Efficient transformation of rice (*Oryza sativa* L.) mediated by *Agrobacterium* and sequence analysis of the boundaries of the T-DNA. *Plant J*. 1994;**6**(2):271–282. <https://doi.org/10.1046/j.1365-313X.1994.6020271.x>

Hong Z, Ueguchi-Tanaka M, Fujioka S, Takatsuto S, Yoshida S, Hasegawa Y, Ashikari M, Kitano H, Matsuoka M. The rice brassinosteroid-deficient dwarf2 mutant, defective in the rice homolog of *Arabidopsis* DIMINUTO/DWARF1, is rescued by the endogenously accumulated alternative bioactive brassinosteroid, dolichosterone. *Plant Cell* 2005;**17**(8):2243–2254. <https://doi.org/10.1105/tpc.105.030973>

Huot B, Yao J, Montgomery B, He S. Growth-defense tradeoffs in plants: a balancing act to optimize fitness. *Mol Plant*. 2014;**7**(8):1267–1287. <https://doi.org/10.1093/mp/issu049>

Kim T-W, Wang Z. Brassinosteroid signal transduction from receptor kinases to transcription factors. *Annu Rev Plant Bio*. 2010;**61**(1):681–704. <https://doi.org/10.1146/annurev.arplant.043008.092057>

Kumar S, Stecher G, Tamura K. MEGA7: molecular evolutionary genetics analysis version 7.0 for bigger datasets. *Mol Biol Evol*. 2016;**33**(7):1870–1874. <https://doi.org/10.1093/molbev/msw054>

Kuusk S, Sohlberg J, Magnus Eklund D, Sundberg E. Functionally redundant SHI family genes regulate *Arabidopsis* gynoecium development in a dose-dependent manner. *Plant J*. 2006;**47**(1):99–111.

- Li Q, Xu F, Chen Z, Teng Z, Sun K, Li X, Yu J, Zhang G, Liang Y, Huang X, et al.** Synergistic interplay of ABA and BR signal in regulating plant growth and adaptation. *Nat Plants*. 2021;7(8):1108–1118. <https://doi.org/10.1038/s41477-021-00959-1>
- Lin R, Ding L, Casola C, Ripoll D, Feschotte C, Wang H.** Transposase-derived transcription factors regulate light signaling in *Arabidopsis*. *Science* 2007;318(5854):1302–1305. <https://doi.org/10.1126/science.1146281>
- Livak K, Schmittgen T.** Analysis of relative gene expression data using real-time quantitative PCR and the $2^{-\Delta\Delta CT}$ method. *Methods* 2001;25(4):402–408. <https://doi.org/10.1006/meth.2001.1262>
- Nambara E, Marion-Poll A.** Abscisic acid biosynthesis and catabolism. *Annu Rev Plant Bio*. 2005;56(1):165–185. <https://doi.org/10.1146/annurev.arplant.56.032604.144046>
- Ning Y, Jantasuriyarat C, Zhao Q, Zhang H, Chen S, Liu J, Liu L, Tang S, Park C, Wang X, et al.** The SINA E3 ligase OsDIS1 negatively regulates drought response in rice. *Plant Physiol*. 2011;157(1):242–255. <https://doi.org/10.1104/pp.111.180893>
- Okushima Y, Fukaki H, Onoda M, Theologis A, Tasaka M.** ARF7 and ARF19 regulate lateral root formation via direct activation of LBD/ASL genes in *Arabidopsis*. *Plant Cell* 2007;19(1):118–130. <https://doi.org/10.1105/tpc.106.047761>
- Raghavendra S, Gonugunta K, Christmann A, Grill E.** ABA perception and signaling. *Trends Plant Sci*. 2010;15(7):395–401. <https://doi.org/10.1016/j.tplants.2010.04.006>
- Ren Y, Wang Y, Liu F, Zhou K, Ding Y, Zhou F, Wang Y, Liu K, Gan L, Ma W, et al.** GLUTELIN PRECURSOR ACCUMULATION3 encodes a regulator of post-Golgi vesicular traffic essential for vacuolar protein sorting in rice endosperm. *Plant Cell* 2014;26(1):410–425. <https://doi.org/10.1105/tpc.113.121376>
- Shen J, Lv B, Luo L, He J, Mao C, Xi D, Ming F.** The NAC-type transcription factor OsNAC2 regulates ABA-dependent genes and abiotic stress tolerance in rice. *Sci Rep*. 2017;7(1):40641. <https://doi.org/10.1038/srep40641>
- Sohlberg J, Myrenäs M, Kuusk S, Lagercrantz U, Kowalczyk M, Sandberg G, Sundberg E.** STY1 regulates auxin homeostasis and affects apical-basal patterning of the *Arabidopsis* gynoecium. *Plant J*. 2006;47(1):112–123.
- Tanabe S, Ashikari M, Fujioka S, Takatsuto S, Yoshida S, Yano M, Yoshimura A, Kitano H, Matsuoka M, Fujisawa Y, et al.** A novel cytochrome P450 is implicated in brassinosteroid biosynthesis via the characterization of a rice dwarf mutant, *dwarf11*, with reduced seed length. *Plant Cell* 2005;17(3):776–790. <https://doi.org/10.1105/tpc.104.024950>
- Tian X, Li X, Zhou W, Ren Y, Wang Z, Liu Z, Tang J, Tong H, Fang J, Bu Q.** Transcription factor OsWRKY53 positively regulates brassinosteroid signaling and plant architecture. *Plant Physiol*. 2017;175(3):1337–1349. <https://doi.org/10.1104/pp.17.00946>
- Tong H, Chu C.** Functional specificities of brassinosteroid and potential utilization for crop improvement. *Trends Plant Sci*. 2018;23(11):1016–1028. <https://doi.org/10.1016/j.tplants.2018.08.007>
- Tong H, Liu L, Jin Y, Du L, Yin Y, Qian Q, Zhu L, Chu C.** DWARF AND LOW-TILLERING acts as a direct downstream target of GSK3/SHAGGY-like kinase to mediate brassinosteroid responses in rice. *Plant Cell* 2012;24(6):2562–2577. <https://doi.org/10.1105/tpc.112.097394>
- Ulmasov T, Hagen G, Guilfoyle T.** Activation and repression of transcription by auxin-response factors. *Proc Natl Acad Sci*. 1999;96(10):5844–5849. <https://doi.org/10.1073/pnas.96.10.5844>
- Vert G, Walcher C, Chory J, Nemhauser J.** Integration of auxin and brassinosteroid pathways by Auxin Response Factor 2. *Proc Natl Acad Sci*. 2008;105(28):9829–9834. <https://doi.org/10.1073/pnas.0803996105>
- Waadt R, Sella C, Hsu P, Takahashi Y, Munemasa S.** Plant hormone regulation of abiotic stress responses. *Nat Rev Mol Cell Biol*. 2022;23(10):680–694. <https://doi.org/10.1038/s41580-022-00479-6>
- Wagner D, Weijers D.** Transcriptional responses to the auxin hormone. *Annu Rev Plant Bio*. 2016;67(1):539–574. <https://doi.org/10.1146/annurev-arplant-043015-112122>
- Wang D, Pei K, Fu Y, Sun Z, Li S, Liu H, Tang K, Han N, Tao Y.** Genome-wide analysis of the auxin response factors (ARF) gene family in rice (*Oryza sativa*). *Gene*. 2007;394(1-2):13–24. <https://doi.org/10.1016/j.gene.2007.01.006>
- Wang H, Tang J, Liu J, Hu J, Liu J, Chen Y, Cai Z, Wang X.** Abscisic acid signaling inhibits brassinosteroid signaling through dampening the dephosphorylation of BIN2 by ABI1 and ABI2. *Mol Plant*. 2018;11(2):315–325. <https://doi.org/10.1016/j.molp.2017.12.013>
- Wang Y, Zhang T, Wang R, Zhao Y.** Recent advances in auxin research in rice and their implications for crop improvement. *J Exp Bot*. 2018b;69(2):255–263. <https://doi.org/10.1093/jxb/erx228>
- Xin P, Yan J, Fan J, Chu J, Yan C.** An improved simplified high-sensitivity quantification method for determining brassinosteroids in different tissues of rice and *Arabidopsis*. *Plant Physiol*. 2013;162(4):2056–2066. <https://doi.org/10.1104/pp.113.221952>
- Yamamoto Y, Kamiya N, Morinaka Y, Matsuoka M, Sazuka T.** Auxin biosynthesis by the YUCCA genes in rice. *Plant Physiol*. 2007;143(3):1362–1371. <https://doi.org/10.1104/pp.106.091561>
- Youssef HM, Eggert K, Koppolu R, Alqudah AM, Poursarebani N, Fazeli A, Sakuma S, Tagiri A, Rutten T, Govind G, et al.** VRS2 regulates hormone-mediated inflorescence patterning in barley. *Nat Genet*. 2017;49(1):157–161.
- Yuan T, Xu H, Zhang Q, Zhang L, Lu Y.** The COP1 target SHI-RELATED SEQUENCES directly activates photomorphogenesis-promoting genes. *Plant Cell*. 2018;30(10):2368–2382.
- Yuo T, Yamashita Y, Kanamori H, Matsumoto T, Lundqvist U, Sato K, Ichii M, Jobling A, Taketa S.** A SHORT INTERNODES (SHI) family transcription factor gene regulates awn elongation and pistil morphology in barley. *J Exp Bot*. 2012;63(14):5223–5232.
- Zg E, Zhang YP, Zhou JH, Wang L.** Mini review roles of the bZIP gene family in rice. *Genet Mol Res*. 2014;13(2):3025–3036. <https://doi.org/10.4238/2014.April.16.11>
- Zhang C, Xu Y, Guo S, Zhu J, Huan Q, Liu H, Wang L, Luo G, Wang X, Chong K.** Dynamics of brassinosteroid response modulated by negative regulator LIC in rice. *Plos Genet*. 2012;8(4):e1002686. <https://doi.org/10.1371/journal.pgen.1002686>
- Zhang H, Zhao Y, Zhu J.** Thriving under stress: how plants balance growth and the stress response. *Dev Cell*. 2020;55(5):529–543. <https://doi.org/10.1016/j.devcel.2020.10.012>
- Zhang L, Ren Y, Lu B, Yang C, Feng Z, Liu Z, Chen J, Ma W, Wang Y, Yu X, et al.** FLOURY ENDOSPERM7 encodes a regulator of starch synthesis and amyloplast development essential for peripheral endosperm development in rice. *J Exp Bot*. 2016a;67(3):633–647. <https://doi.org/10.1093/jxb/erv469>
- Zhang S, Wu T, Liu S, Liu X, Jiang L, Wan J.** Disruption of OsARF19 is critical for floral organ development and plant architecture in rice (*Oryza sativa* L.). *Plant Mol Biol Report*. 2016b;34(4):748–760. <https://doi.org/10.1007/s11105-015-0962-y>
- Zhang Y, Su J, Duan S, Ao Y, Dai J, Liu J, Wang P, Li Y, Liu B, Feng D, et al.** A highly efficient rice green tissue protoplast system for transient gene expression and studying light/chloroplast-related processes. *Plant Methods* 2011;7(1):30. <https://doi.org/10.1186/1746-4811-7-30>
- Zhao X, Dou L, Gong Z, Wang X, Mao T.** BES1 Hinders ABSCISIC ACID INSENSITIVE5 and promotes seed germination in *Arabidopsis*. *New Phytol*. 2019;221(2):908–918. <https://doi.org/10.1111/nph.15437>
- Zhao Y.** Auxin biosynthesis and its role in plant development. *Annu Rev Plant Bio*. 2010;61(1):49–64. <https://doi.org/10.1146/annurev-arplant-042809-112308>